GM-CSF regulates intimal cell proliferation in nascent atherosclerotic lesions

Su-Ning Zhu,[1] Mian Chen,[1] Jenny Jongstra-Bilen,[1,2,3] and Myron I. Cybulsky[1,2]

[1]Toronto General Research Institute, University Health Network, Toronto, Ontario M5G 2C4, Canada
[2]Department of Laboratory Medicine and Pathobiology and [3]Department of Immunology, University of Toronto, Toronto, Ontario M5S 1A8, Canada

The contribution of intimal cell proliferation to the formation of early atherosclerotic lesions is poorly understood. We combined 5-bromo-2′-deoxyuridine pulse labeling with sensitive en face immunoconfocal microscopy analysis, and quantified intimal cell proliferation and Ly-6C^{high} monocyte recruitment in low density lipoprotein receptor–null mice. Cell proliferation begins in nascent lesions preferentially at their periphery, and proliferating cells accumulate in lesions over time. Although intimal cell proliferation increases in parallel to monocyte recruitment as lesions grow, proliferation continues when monocyte recruitment is inhibited. The majority of proliferating intimal cells are dendritic cells expressing CD11c and major histocompatibility complex class II and 33D1, but not CD11b. Systemic injection of granulocyte/macrophage colony-stimulating factor (GM-CSF) markedly increased cell proliferation in early lesions, whereas function-blocking anti–GM-CSF antibody inhibited proliferation. These findings establish GM-CSF as a key regulator of intimal cell proliferation in lesions, and demonstrate that both proliferation and monocyte recruitment contribute to the inception of atherosclerosis.

CORRESPONDENCE
Myron Cybulsky:
myron.cybulsky@utoronto.ca

Abbreviations used: *Apoe*, apolipoprotein E; CRD, cholesterol-rich diet; GC, greater curvature; GMRα, GM-CSF receptor α chain; LC, lesser curvature; LDL, low density lipoprotein; *Ldlr*, LDL receptor; MFI, mean fluorescence intensity; MHC II, MHC class II; PTx, pertussis toxin; SCD, standard chow diet.

In atherosclerosis, serum lipoproteins, particularly low density lipoprotein (LDL), accumulate in the arterial intima through binding to matrix proteoglycans (Skålén et al., 2002) and undergo oxidative modification. Blood monocytes are recruited into these regions of the intima, differentiate into macrophages or DCs, and internalize oxidatively modified lipoproteins via scavenger receptors or by macropinocytosis (for review see Moore and Freeman, 2006). BM-derived cells accumulate in early mouse atherosclerotic lesions (Mullick et al., 2008), and monocyte recruitment persists in advanced lesions (Swirski et al., 2006; Tacke et al., 2007).

Circulating monocytes consist of at least two subpopulations, with distinct expression of cell-surface markers, chemokine receptors, and functions during inflammatory responses (Grage-Griebenow et al., 2001; Geissmann et al., 2003). In mice, the Ly-6C^{high} subset is elevated during hypercholesterolemia and is preferentially recruited to atherosclerotic lesions (Swirski et al., 2007; Tacke et al., 2007). Ly-6C^{high} monocytes express abundant L-selectin and multiple chemokine receptors, including CCR2, but relatively low levels of CX3CR1. Ly-6C^{low} monocytes express higher levels of CX3CR1, and low to nondetectable levels of most chemokine receptors, L-selectin and Ly-6C. Thus, it is intriguing that recruitment of Ly-6C^{high} monocytes to lesions is dependent on CCR2, CCR5, and CX3CR1, whereas recruitment of Ly-6C^{low} monocytes is independent of CX3CR1 and dependent on CCR5, which is up-regulated in hypercholesterolemic mice (Tacke et al., 2007).

Fatty streaks are composed almost entirely of myeloid foam cells, and their formation and lateral expansion are critically dependent on monocytes/macrophages. This was demonstrated using osteopetrotic mice that have a point mutation that disrupts M-CSF and are deficient in circulating monocytes, tissue macrophages, and osteoclasts. Osteopetrotic mice are highly protected from atherosclerosis in the setting of hypercholesterolemia (Smith et al., 1995; Qiao et al., 1997), and these studies implicate monocytes and their progeny as key

The Rockefeller University Press $30.00
J. Exp. Med. Vol. 206 No. 10 2141-2149
www.jem.org/cgi/doi/10.1084/jem.20090866

cells in lesion development. In contrast to M-CSF, deficiency of GM-CSF has no significant effects on circulating monocytes or tissue macrophages, and variable effects on mouse atherosclerotic lesion formation (Ditiatkovski et al., 2006; Shaposhnik et al., 2007). An interesting feature in the setting of GM-CSF deficiency is a decrease of $CD11c^+$ cells in lesions (Shaposhnik et al., 2007).

The biology of macrophages and DCs in atherosclerotic lesions is complex. These cells can proliferate or undergo apoptosis, and both processes have been observed primarily in advanced human and experimental lesions (Rosenfeld and Ross, 1990; Orekhov et al., 1998; Merched et al., 2003) and in a vascular occlusion model in hypercholesterolemic apolipoprotein E–deficient (*Apoe*$^{-/-}$) mice (Lessner et al., 2002). The prevailing opinion is that monocyte recruitment accounts for the formation of early lesions, and the relationship of proliferation to monocyte recruitment is not understood. A key impediment has been the lack of a sensitive approach to study cell proliferation and monocyte recruitment in early lesions. We used BrdU pulse labeling combined with en face confocal microscopy of the mouse aorta to detect cell proliferation and Ly-$6C^{high}$ monocyte recruitment, and localize them with respect to lipid accumulation in the intima. We found that intimal cell proliferation begins in nascent lesions preferentially at the periphery, increases as lesions progress in parallel to monocyte recruitment, primarily involves DCs, and is dependent on GM-CSF but not monocyte recruitment.

RESULTS AND DISCUSSION

BrdU pulse labeling preferentially labels Ly-$6C^{high}$ blood monocytes

BrdU is stably incorporated into the DNA of cells during the S phase of the cell cycle. Pulse labeling is achieved because injected BrdU is cleared from the plasma within hours (Kriss and Revesz, 1962). BrdU labels proliferating monocyte precursors in the BM, and labeled monocytes appear in the circulation after 4–6 h (Goto et al., 2003; Jongstra-Bilen et al., 2006). We used flow cytometry to investigate BrdU labeling of BM and blood monocyte subsets in wild-type C57BL/6 mice (Fig. 1 a). $BrdU^+$ Ly-$6C^{high}CD115^{high}$ cells were detected in the BM at 2 h, increased, and reached a plateau at 12 h (Fig. 1 b). In the blood, $BrdU^+$ Ly-$6C^{high}$ monocytes were not detected within 6 h but increased rapidly thereafter and reached a plateau at 12–24 h (Fig. 1 b), at which time 35–45% of circulating blood Ly-$6C^{high}$ monocytes were $BrdU^+$. Ly-$6C^{neg}CD115^{high}$ BM cells and blood monocytes did not stain for BrdU. The mean fluorescence intensity (MFI) of BM BrdU-labeled Ly-$6C^{high}CD115^{high}$ cells declined over time, consistent with ongoing rapid proliferation of monocyte precursors (Fig. 1 c). In contrast, the MFI of $BrdU^+$ Ly-$6C^{high}$ blood monocytes remained relatively stable over 24 h.

Wild-type mice are resistant to developing diet-induced hypercholesterolemia and atherosclerosis. In atherosclerosis-susceptible *Apoe*$^{-/-}$ mice, prolonged and marked hypercholesterolemia as a result of feeding a high fat diet for 12–25 wk induced a substantial increase in the number of circulating Ly-$6C^{high}$ monocytes, which are preferentially recruited to plaques (Swirski et al., 2007; Tacke et al., 2007). The effects of short-term hypercholesterolemia on monocyte release from the BM and circulating monocyte levels is unknown. We fed LDL receptor–null (*Ldlr*$^{-/-}$) mice a cholesterol-rich diet (CRD) for just 2 wk and found that the number of Ly-$6C^{high}$ blood monocytes was increased 2.9-fold (Fig. 1 d). In contrast, circulating Ly-$6C^{neg}$ monocytes were not significantly increased by hypercholesterolemia (Fig. 1 d). There was a trend toward higher BrdU labeling of Ly-$6C^{high}$ blood monocytes at 12, 18, and 24 h in hypercholesterolemic mice, and a statistically significant difference ($P < 0.03$) between hypercholesterolemic and normocholesterolemic mice was found when data from these time points were combined (Fig. 1 e).

Proliferation of intimal leukocytes increases progressively from the inception of atherosclerosis in parallel to recruitment of BM-derived Ly-$6C^{high}$ monocytes

Feeding *Ldlr*$^{-/-}$ mice a CRD initiates a marked hypercholesterolemia and atherosclerotic lesion formation throughout the aorta (Ishibashi et al., 1994a; Lichtman et al., 1999). As early as 1 wk after CRD feeding, nascent lesions were detected in the lesser curvature (LC) of the *Ldlr*$^{-/-}$ ascending aorta, and lesion surface area increased progressively with time (Fig. 2 a). Cell proliferation in the ascending aortic intima was examined 2 h after injection of BrdU, a time point when $BrdU^+$ monocytes were not detected in the circulation (Fig. 1 e). $BrdU^+$ nuclei were also quantified 24 h after BrdU injection when proliferating intimal cells as well as BM-derived BrdU-labeled Ly-$6C^{high}$ monocytes recruited from the blood are detected. As we reported previously (Jongstra-Bilen et al., 2006), in the ascending aorta of normal C57BL/6 mice (*Ldlr*$^{+/+}$), we found very low proliferation at 2 h only in the LC (0.5 $BrdU^+$ nuclei; Fig. 2 b). At 24 h, $BrdU^+$ nuclei increased by 20-fold to 10.3 ± 2.3 nuclei, which represents mostly recruited BrdU-labeled Ly-$6C^{high}$ monocytes and is consistent with our previous findings (Jongstra-Bilen et al., 2006). In *Ldlr*$^{-/-}$ mice fed a standard chow diet (SCD; Fig. 2 b, time point 0), the numbers of $BrdU^+$ nuclei at 2 and 24 h were virtually identical to wild-type C57BL/6 mice (0.5 ± 0.3 and 10 ± 2, respectively), indicating relatively comparable baseline rates of cell proliferation and monocyte recruitment to the intima. After switching *Ldlr*$^{-/-}$ mice to a CRD, the number of $BrdU^+$ nuclei at 2 and 24 h progressively increased, which demonstrates a parallel increase in both intimal cell proliferation and monocyte recruitment from the inception of atherosclerosis. At 2 wk of CRD, intimal cell proliferation increased by 40-fold relative to C57BL/6 and *Ldlr*$^{-/-}$ mice fed a SCD, and the abundance of $BrdU^+$ nuclei detected at 24 h increased by approximately 8-fold.

All $BrdU^+$ nuclei were located in the LC (Fig. 2, d and e) and many ($88 \pm 4\%$ and $66 \pm 12\%$ at 2 and 24 h, respectively) were at borders of lesions (Fig. 2, c and d), suggesting that cell proliferation and monocyte recruitment occur

in similar regions. Proliferating intimal cells at borders of lesions were often adjacent to cells containing lipid droplets, and their nuclei extended below the endothelial cell monolayer (Fig. S1, a–c).

Proliferating intimal cells accumulate in 2-wk atherosclerotic lesions

BrdU labeling in lesions was initially studied within 6 h of BrdU injection, when minimal BrdU$^+$ monocytes are released from

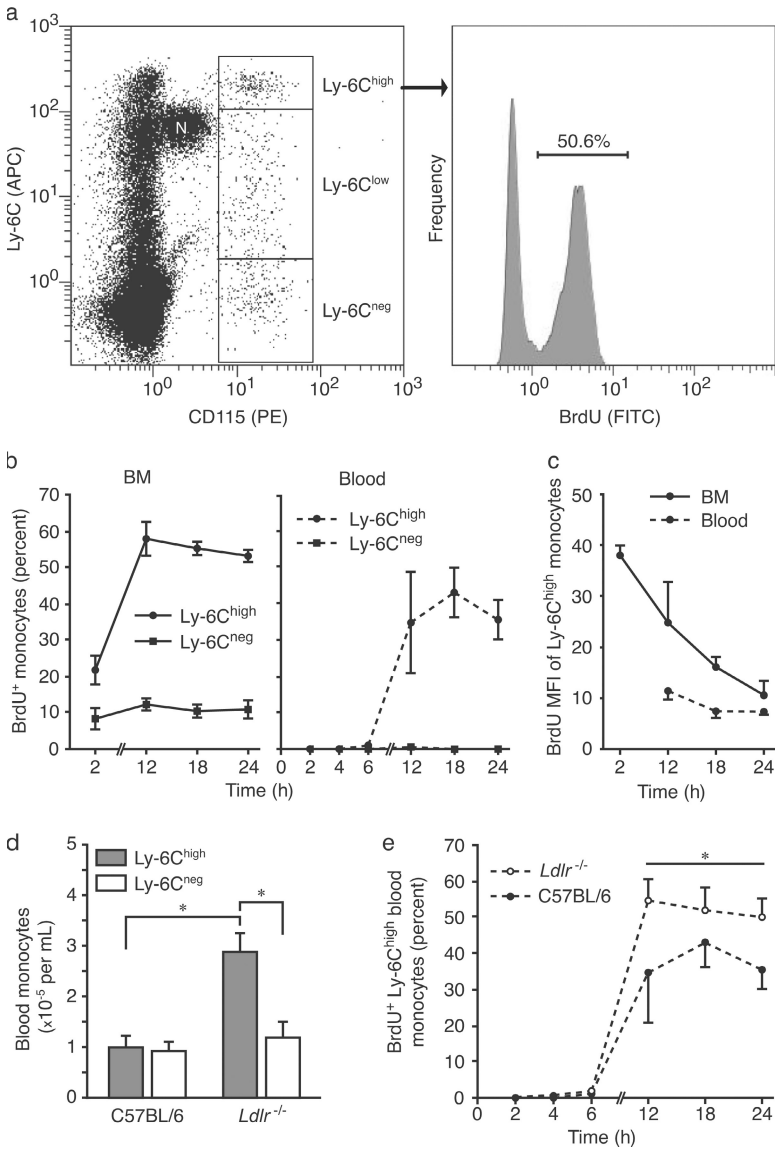

Figure 1. Analysis of BrdU pulse-labeled monocyte subpopulations in the BM and blood using flow cytometry. (a, left) A dot plot of a blood sample from a C57BL/6 mouse obtained 18 h after BrdU injection illustrates identification of monocyte subsets. Typically, >85% of events were gated in forward versus side scatter analysis (not depicted). Monocytes expressed high levels of CD115$^+$, and subpopulations were identified based on high, low, and negative (neg) expression levels of Ly-6C. Neutrophils (N), expressing low levels of CD115 and intermediate levels of Ly-6C, served as a landmark for setting the Ly-6C^{high} gate. (right) A histogram of BrdU fluorescence gated on the Ly-6C^{high} cells indicated that 50.6% were BrdU$^+$. Representative data from one out of three independent experiments is shown. (b) The percentages of BrdU$^+$ Ly-6C^{high} and Ly-6C^{neg} monocytes in the BM (left) and blood (right) of C57BL/6 mice are plotted at different time points after BrdU injection. (c) A time course shows the MFI of BrdU$^+$ Ly-6C^{high} monocytes in the BM and blood. In b and c, three independent experiments were performed and means ± SEM were derived from three mice per time point. (d) The absolute numbers of Ly-6C^{high} and Ly-6C^{neg} monocytes in the blood of C57BL/6 mice and *Ldlr*$^{-/-}$ mice fed a CRD for 2 wk are plotted. They were derived from total blood leukocyte counts, and the percentage of each monocyte subpopulation was determined by flow cytometry. The total blood leukocyte count was elevated 1.5-fold in *Ldlr*$^{-/-}$ relative to C57BL/6 mice (8.94 ± 0.75 vs. 5.8 ± 0.38 × 10^6 cells/ml; three and two independent experiments, respectively). Means ± SEM were derived from eight mice per genotype (*, $P < 0.005$). (e) Percentage of BrdU$^+$ Ly-6C^{high} monocytes in the blood after BrdU pulse labeling of C57BL/6 mice and *Ldlr*$^{-/-}$ mice fed a CRD for 2 wk (three independent experiments for each genotype with means ± SEM derived from three mice per time point). The asterisk indicates a statistically significant difference ($P < 0.03$) between hypercholesterolemic and normocholesterolemic mice when data from the 12, 18, and 24 h time points were combined (53.3 ± 3.2% vs. 38.5 ± 4.8%).

the BM (Fig. 1 e). Intimal BrdU$^+$ nuclei were detected at 1 h, increased at 2 and 3 h, and then remained stable (Fig. S1 d). This suggests that the BrdU labeling window is <3 h. Another possibility is that labeled intimal cells complete mitosis within 3 h. Consistent with this, BrdU$^+$ nuclear doublets that likely represent daughter cells also increased within 3 h (Fig. S1, e and f).

Proliferating intimal cells may divide to produce two daughter cells or, alternatively, may undergo apoptosis. The

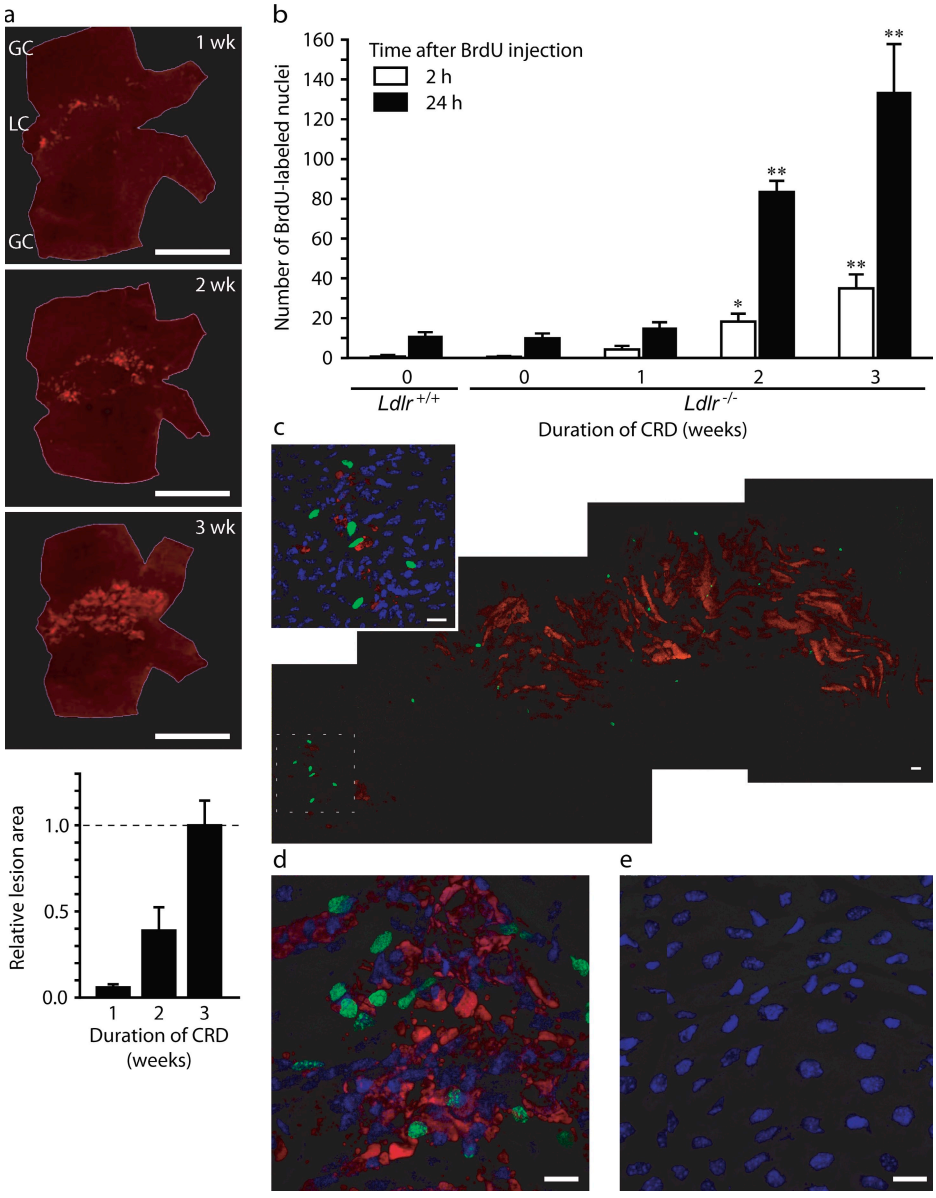

Figure 2. Quantification of lipid accumulation, intimal cell proliferation, and monocyte recruitment during the initiation of atherosclerosis. (a) En face fluorescent images of ascending aortas from *Ldlr*$^{-/-}$ mice fed a CRD for 1, 2, or 3 wk. Intimal lipid accumulation was visualized (red; top), and the lesion areas relative to the value for the 3-wk CRD group (dashed line) were determined (bottom). Means ± SEM were derived from 4 (1 wk), 22 (2 wk), and 6 (3 wk) mice studied in 2, 11, and 3 independent experiments, respectively. A representative image is shown for each time point. Note that lipid accumulation was detected in the LC but not in the GC, or in *Ldlr*$^{-/-}$ mice fed SCD (not depicted). (b) Intimal BrdU$^+$ nuclei were enumerated at 2 and 24 h after BrdU pulse labeling in C57BL/6 mice (*Ldlr*$^{+/+}$) fed SCD or *Ldlr*$^{-/-}$ mice fed a CRD (0–3 wk). The entire surface of the ascending aorta above the aortic valve was scanned by en face confocal microscopy, but BrdU$^+$ nuclei were detected only in the LC. For each time point, four to seven independent experiments were performed, and means ± SEM were derived from four to seven mice (*, $P < 0.05$; **, $P < 0.01$ relative to *Ldlr*$^{-/-}$ mice fed SCD, i.e., 0 wk of CRD). (c) A composite of en face images taken with a 16× objective shows the entire oil red O–stained lesion area (red) in the LC of the ascending aortic arch harvested from an *Ldlr*$^{-/-}$ mouse that was fed a CRD for 2 wk and pulsed for 2 h with BrdU. BrdU$^+$ nuclei (green) are primarily at the periphery of the lesion. Inset (top left) shows a high power image of the region indicated with dashed lines. Nuclei are blue. (d and e) En face confocal images of the ascending aortic arch harvested from an *Ldlr*$^{-/-}$ mouse fed CRD for 2 wk and pulsed with BrdU for 24 h. BrdU$^+$ nuclei and lipid accumulated in the LC (d) but not in the GC (e). Images in c, d, and e are representative of at least four independent experiments. Bars: (a) 1 mm; (c–e) 20 µm.

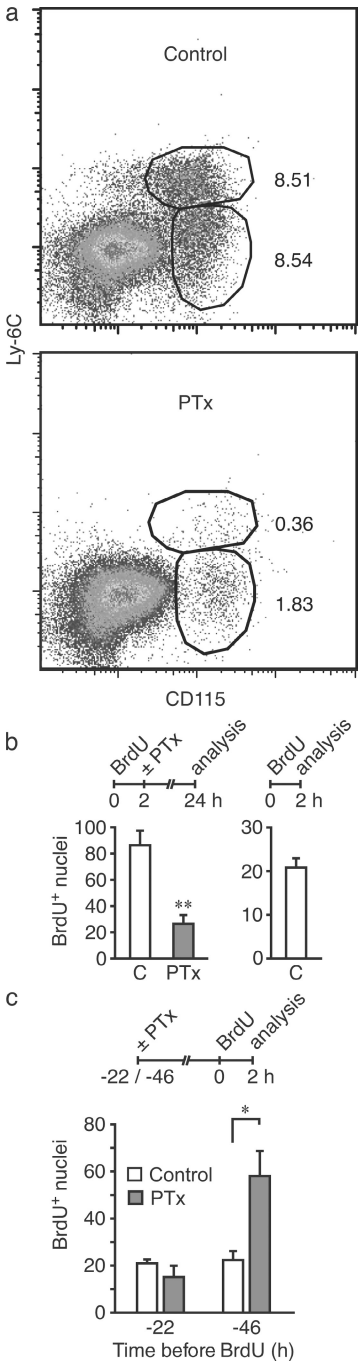

Figure 3. PTx blockade of monocyte recruitment reveals that proliferating intimal cells accumulate in 2-wk lesions, and intimal cell proliferation is independent of monocyte recruitment. (a) Flow cytometry plots of peritoneal exudate cells harvested 24 h after i.p. thioglycollate injection of control and PTx-treated mice (percentages are indicated). Representative data from five mice per group studied in two independent experiments are shown. Additional details are provided in Fig. S2. (b) *Ldlr*$^{-/-}$ mice fed a CRD for 2 wk were injected with BrdU at 2 h before treatment with PTx or PBS (C, control). Aortas were harvested 24 h (left) and 2 h (right) after BrdU injection, and BrdU$^+$ nuclei were enumerated. (c) *Ldlr*$^{-/-}$ mice fed a CRD for 2 wk were injected with PTx, and BrdU pulse labeling was performed 22 or 46 h later. Aortas were harvested after 2 h, and BrdU$^+$ nuclei were enumerated. In b and c, four independent experiments were performed at each time point, and means ± SEM were derived from four mice per group. *, $P < 0.05$ relative to C; **, $P < 0.01$.

fate of proliferating intimal cells was investigated by inhibiting blood monocyte recruitment with pertussis toxin (PTx). PTx inactivates Gαi chemokine receptors and has been used in vivo to study the contribution of chemokine receptors versus E-selectin–triggered integrin activation in neutrophil recruitment to the inflamed peritoneal cavity (Smith et al., 2004). We found that PTx markedly diminished monocyte recruitment at 24 h to thioglycollate-inflamed peritoneal cavity despite a marked increase in circulating myeloid cells (Fig. 3 a and Fig. S2). In contrast, PTx reduced but did not eliminate neutrophil recruitment, consistent with a previous report (Smith et al., 2004). These data illustrate an important difference in monocytes versus neutrophil signaling. As was shown previously, neutrophil binding to E-selectin induces a compensatory signaling pathway that bypasses $G\alpha_i$ signaling irreversibly blocked by PTx, whereas our data suggest that this compensatory pathway is not operative in monocytes.

In *Ldlr*$^{-/-}$ mice fed a CRD for 2 wk, PTx significantly diminished the number of BrdU$^+$ nuclei at 24 h from 86 ± 10 to 26 ± 12 (Fig. 3 b), consistent with PTx blockade of monocyte recruitment. In a parallel experiment, 21 ± 2 BrdU$^+$ nuclei representing intimal cells were detected at 2 h. Comparable BrdU$^+$ nuclei (26 ± 12) were detected in the PTx experiment at 24 h, suggesting that proliferating intimal cells persist and accumulate in lesions.

Intimal cell proliferation is independent of monocyte recruitment

Intimal cell proliferation in 2-wk lesions was determined by 2-h BrdU labeling after inhibition of monocyte recruitment for 22 or 46 h with PTx. Proliferation was not decreased by PTx at 22–24 h and, in fact, increased at 46–48 h (Fig. 3 c), which may represent a compensatory increase in cell proliferation in response to diminished blood monocyte recruitment. These data reveal that proliferating intimal cells are not newly recruited blood monocytes.

Proliferating intimal cells express DC markers

Immunostaining for various leukocyte markers was performed to determine the phenotype of BrdU$^+$ cells in atherosclerotic lesions. The majority of foam cells in 2-wk lesions are CD11c$^+$ and CD68$^+$, whereas CD11b$^+$ cells are located in clusters (Fig. S3). After 2 or 24 h of BrdU labeling, >90% of BrdU$^+$ cells expressed CD45, a pan-leukocyte marker (Fig. 4 b). BrdU$^+$ cells costained predominantly with CD11b 24 h after labeling (Fig. 4, a and b), consistent with recruitment to lesions of Ly-6C^{high} blood monocytes, which are CD11b$^+$. More than 90% of proliferating cells (2 h of BrdU labeling) costained for CD11c, a DC marker, and >60% of BrdU$^+$ cells expressed CD11c at 24 h, consistent with survival of proliferating CD11c$^+$ cells.

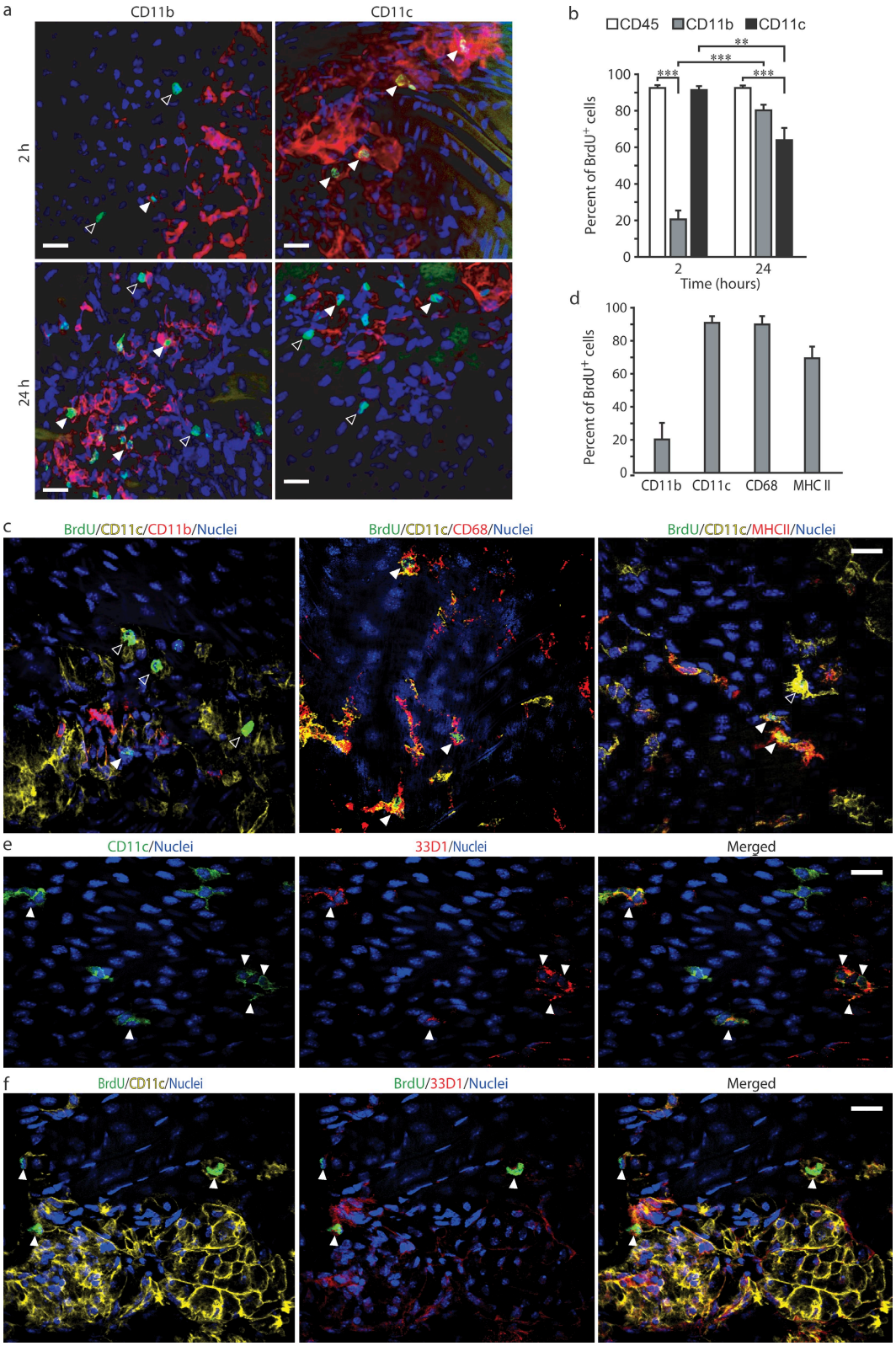

Figure 4. Expression of leukocyte markers by BrdU+ cells in early atherosclerotic lesions. (a and b) *Ldlr*$^{-/-}$ mice fed a CRD for 2 wk were injected with BrdU at 2 or 24 h before harvesting of the ascending aorta. (a) Immunostaining for BrdU (green) was performed in conjunction with CD11b (red), CD11c (red), or CD45 (not depicted), and tissues were examined by en face confocal microscopy. Nuclei are blue. Arrowheads indicate representative BrdU+ cells that costained with CD11b or CD11c (closed) and those that were not costained (open). (b) Quantitative analysis of BrdU+ intimal cells that

The expression of additional myeloid and DC markers by proliferating cells in 2-wk lesions was evaluated. 2 h after BrdU labeling, most $BrdU^+CD11c^+$ cells costained with CD68, a marker expressed by monocytes, macrophages, and DCs (Fig. 4, c and d; and Fig. S4). Relatively low costaining with $CD11b^+$ was confirmed. Many $BrdU^+CD11c^+$ cells costained with MHC class II (MHC II; Fig. 4, c and d; and Fig. S4), which is expressed by DCs, and with 33D1 (Fig. 4 f), a mAb that specifically targets mouse DCs (Nussenzweig et al., 1982; Xu et al., 2007). 33D1 stained resident intimal DCs in the normal mouse aorta (Fig. 4 e). Collectively, our data indicate that the majority of proliferating intimal cells in early atherosclerotic lesions express DC markers and, thus, may be capable of DC functions analogous to intimal DCs in the normal intima (Choi et al., 2009). Proliferating cells in early lesions may originate from intimal DCs residing in atherosclerosis-predisposed regions of the normal intima (Jongstra-Bilen et al., 2006; Choi et al., 2009) and/or recruited monocytes that differentiated in lesions to express DC markers after several days.

GM-CSF is a critical regulator of cell proliferation in early atherosclerotic lesions

GM-CSF is a myeloid growth factor that induces DC differentiation from BM precursors and monocytes, and regulates the properties of mature myeloid cells in inflammation (Hamilton and Anderson, 2004). Modified LDL induces endothelial cell expression of GM-CSF (Rajavashisth et al., 1990), and GM-CSF down-regulates serum cholesterol while up-regulating VLDL receptor mRNA expression (Ishibashi et al., 1994b). GM-CSF deficiency has variable effects on mouse atherosclerosis. In $Ldlr^{-/-}$ mice, lesions were decreased (Shaposhnik et al., 2007), whereas in $Apoe^{-/-}$ mice they were increased (Ditiatkovski et al., 2006). Because the majority of proliferating cells in early lesions are $CD11c^+$ (Fig. 3) and GM-CSF deficiency results in decreased $CD11c^+$ cells in lesions (Shaposhnik et al., 2007), we investigated whether GM-CSF regulates cell proliferation in atherosclerotic lesions.

Initial experiments used real-time PCR to investigate mRNA expression of the GM-CSF receptor α chain (GMRα) in 2-wk-old lesions of $Ldlr^{-/-}$ mice. GMRα is specific for GM-CSF, unlike the β chain that is shared by IL-3 and IL-5 (Rosas et al., 2007). The LC intima of the ascending aortic arch, which contains lesions, was compared with the nondiseased greater curvature (GC), a region that is protected from atherosclerotic lesion development. Expression of GMRα was markedly elevated in lesions relative to the uninvolved GC intima (Fig. 5 a). There was also enrichment of DCs and myeloid cell markers (CD11c and CD68) in lesions, but expressions of T cell (CD3), smooth muscle cell (SM22α), and endothelial cell (CD31 and intercellular adhesion molecule 2) markers were comparable. Having established that GMRα is expressed in 2-wk lesions, two complementary experiments directly evaluated the role of GM-CSF in intimal cell proliferation. Injection of mouse GM-CSF increased the abundance of $BrdU^+$ nuclei by 2.7-fold in 2-wk intimal lesions (Fig. 5 b), indicating that many cells in lesions are capable of proliferating after exposure to GM-CSF. In this experiment, $BrdU^+$ leukocytes were not detected in the circulation. Injection of a function-blocking antibody to GM-CSF reduced the number of proliferating cells in lesions by 4.8-fold (Fig. 5 c). Collectively, our data demonstrate that GM-CSF is critical for intimal cell proliferation in early lesions.

Germline genetic manipulations in mouse models are used to investigate molecular atherogenic mechanisms, yet analysis of atherosclerotic lesions in mice typically consists of lesion burden assessment (by staining for accumulated intimal lipid) and evaluation of cell/matrix composition using histological approaches. Leukocyte recruitment and intimal cell proliferation or death can independently result in differences in lesion burden. This study illustrates a practical, sensitive, and reproducible approach for quantifying cellular events in atherosclerosis. BrdU pulse labeling combined with en face confocal microscopy provides quantitative information on intimal cell proliferation, as well as recruitment of Ly-$6C^{high}$ blood monocytes within a 24-h window. Using this approach, we showed that proliferation of intimal cells and recruitment of BM-derived Ly-$6C^{high}$ monocytes increase progressively from the inception of atherosclerosis. Experiments with PTx suggested that the two processes occur independently of each other and raise the possibility that blockade of recruitment or proliferation individually may result in a compensatory response. Thus, for effective therapy it may be necessary to target both processes. Previously, GM-CSF was reported to function in the differentiation of monocytes to DCs (Chapuis et al., 1997; Daro et al., 2000) and in the proliferation of mouse DC precursors (Inaba et al., 1992). Our current data support an important role for GM-CSF in mediating intimal DC proliferation in early atherosclerotic lesions and suggest that it may be prudent to block functions of this cytokine when administering a therapy for early atherosclerosis that targets monocyte recruitment.

costained with CD45, CD11b, or CD11c at 2 and 24 h after labeling. Data are expressed as the percentage of total $BrdU^+$ cells. (c and d) $Ldlr^{-/-}$ mice fed a CRD for 2 wk were injected with BrdU 2 h before harvesting of the ascending aorta. (c) Immunostaining for BrdU (green) and CD11c (yellow) was performed in conjunction with CD11b, CD68, or MHC II (red). Closed arrowheads indicate $BrdU^+$ cells that costained with CD11c and CD11b, CD68, or MHC II; open arrowheads indicate $BrdU^+$ cells costained only with CD11c. (d) Quantitative analysis of $BrdU^+$ intimal cells that costained with the indicated markers. (e) Images of the ascending arch LC from normal C57BL/6 mice costained for CD11c (green) and 33D1 (red; arrowheads). (f) Images of the ascending arch LC from $Ldlr^{-/-}$ mice fed a CRD for 2 wk and injected with BrdU at 2 h before harvesting costained for BrdU (green), CD11c (yellow), and 33D1 (red; arrowheads). All images are representative of four independent experiments. In b and d, means ± SEM of four independent experiments are plotted (four mice per group; **, $P < 0.01$; ***, $P < 0.001$). Bars, 20 µm.

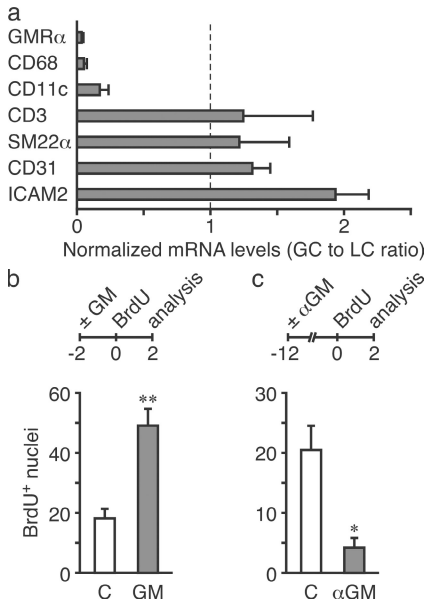

Figure 5. Expression of GMRα by intimal cells in the LC of the aortic arch and regulation of intimal cell proliferation by GM-CSF in early lesions. (a) Analysis of GMRα and cell marker gene (CD68, myeloid cells; CD11c, DCs; CD3, T cells; SM22α, smooth muscle cells; CD31 and intercellular adhesion molecule 2 [ICAM2], endothelial cells) mRNA levels by real-time PCR in intimal cells harvested from the GC and LC of ascending aortic arches of *Ldlr*$^{-/-}$ mice fed a CRD for 2 wk. Values represent the GC to LC ratios. The dashed line (value of 1) indicates equal expression in the GC and LC, and ratios of <1 indicate higher expression levels in the LC. In each experiment, RNA from three aortas was pooled and means ± SEM of three independent experiments are plotted. (b and c) *Ldlr*$^{-/-}$ mice fed a CRD for 2 wk were injected i.v. with mouse rGM-CSF (GM) or buffer (C, control) and BrdU as indicated in b, or mAb to mouse GM-CSF (αGM) or isotype control (C) and BrdU as indicated in c. BrdU$^+$ nuclei in the ascending aorta were enumerated from en face confocal images. Means ± SEM were derived from seven control and four GM-treated mice (b), and four control and four αGM-treated mice (c). *, $P < 0.05$; **, $P < 0.01$.

MATERIALS AND METHODS

Mice, BrdU labeling, and treatment with PTx, GM-CSF, or antibody to GM-CSF. Wild-type C57BL/6 and *Ldlr*$^{-/-}$ mice backcrossed >10 generations into the C57BL/6 background obtained from the Jackson Laboratory were bred. All procedures were approved by the University Health Network Animal Care Committee. At 10–12 wk of age, *Ldlr*$^{-/-}$ males or females were switched to a 1.25% cholesterol diet (Lichtman et al., 1999). In BrdU labeling experiments, mice received a single 0.2-ml i.v. injection of 2 mg BrdU in PBS (BD). In some experiments, BrdU labeling was performed in conjunction with i.v. injection of 2 μg PTx in PBS (Sigma-Aldrich), 0.01 μg/g of body weight of mouse rGM-CSF in 1% FBS (R&D Systems), or 100 μg anti–mouse GM-CSF (functional grade MP1-22E9; eBioscience). Controls were injected with 0.2 ml PBS, 1% FBS, or isotype control rat IgG2a. Peritonitis was induced with 4% thioglycollate (1 ml i.p.; Difco).

Flow cytometry studies of BrdU-injected mice. Leukocytes obtained from blood or BM of the femur and tibia were stained with PE–anti-CD115 plus biotin–anti–Ly-6C (Biomedicals AG) or biotin–anti-CD19 (BD) mAbs and streptavidin-allophycocyanin (eBioscience). They were then fixed and permeabilized, and DNA was digested with DNase I (Invitrogen) and stained with FITC–anti-BrdU (BrdU detection kit; BD). Data were acquired with a flow cytometer (Cytomics FC500 MPL; Beckman Coulter) and analyzed using FlowJo analysis software (version 7.2.2; Tree Star, Inc.). A hemocytometer (Bright-Line; Hausser Scientific) was used to determine the concentration of blood leukocytes.

En face confocal microscopy of aortas from BrdU-injected mice. Aortas were harvested after perfusion fixation (4% paraformaldehyde, 100 mmHg), and the surrounding adipose tissue was dissected after further fixation for 1 h. For detection of BrdU-labeled intimal cells, aortas were permeabilized (0.5% Triton X-100 for 15 min) and incubated sequentially with 0.3% H_2O_2 (30 min), DNase I (1.5 h at 37°C), FITC-conjugated anti-BrdU (18 h at 4°C), horseradish peroxidase (HRP)–conjugated anti-FITC (1:300 dilution for 1 h; Abcam), and FITC-tyramide (PerkinElmer). Lipid accumulated in lesions was detected by oil red O (Sigma-Aldrich) staining (Lichtman et al., 1999), and nuclei were counterstained with 2 μg/ml Hoechst 33342 (Invitrogen).

For immunophenotyping of BrdU$^+$ cells, aortas were incubated overnight with FITC–anti-BrdU and biotinylated mAb to CD11b (BD), CD11c, CD45 (eBioscience), 33D1 (BD), or CD68 (AbD Serotec). mAbs to CD11b, CD11c, and CD45 were detected with streptavidin-HRP (1:300 dilution) and cyanine 3–tyramide (PerkinElmer), and others were detected with streptavidin-PE. PE–anti–MHC II (BD) and Alexa Fluor 647–anti-CD11c (BioLegend) were also used. A confocal microscope (FV-1000; Olympus) with a 60× (NA 1.4) oil objective was used to acquire images.

Real-time PCR. Enzymatic harvesting of intimal cells, reverse transcription real-time PCR (SYBR green– or FAM-labeled GM-CSF2Rα TaqMan MGB probe; Mm00438331_g1; ABI Prism 7900HT; Applied Biosystems), and normalization of data were performed as previously described (Jongstra-Bilen et al., 2006).

Statistical analyses. Differences between two groups were determined by an unpaired two-tailed *t* test and analysis of variance followed by Tukey-Kramer multiple comparison tests were used to compare multiple groups.

Online supplemental material. Fig. S1 shows the location of proliferating intimal BrdU$^+$ cells (a–c), and the time course of proliferating BrdU$^+$ nuclei and BrdU$^+$ nuclear doublets (d–f) in 2-wk lesions. Fig. S2 depicts flow cytometry analysis of the peritoneal exudates and blood of PTx-treated and control mice. Fig. S3 shows the distribution of BrdU$^+$CD11c$^+$ proliferating intimal cells costained with CD68 or CD11b in 2-wk lesions. Fig. S4 depicts costaining of BrdU$^+$CD11c$^+$ proliferating intimal cells with MHC II and CD68. Online supplemental material is available at http://www.jem.org/cgi/content/full/jem.20090866/DC1.

We thank the Banting and Best Diabetes Centre and the Toronto General Research Institute for contributing to the purchase of the ABI Prism 7900HT real-time PCR machine.

This research was supported by the Heart and Stroke Foundation of Ontario (HSFO; grant T-6107). M.I. Cybulsky is a Career Investigator of the HSFO and a member of the Heart and Stroke/Richard Lewar Centre of Excellence at the University of Toronto.

The authors have no conflicting financial interests.

Submitted: 20 April 2009
Accepted: 20 August 2009

REFERENCES

Chapuis, F., M. Rosenzwajg, M. Yagello, M. Ekman, P. Biberfeld, and J.C. Gluckman. 1997. Differentiation of human dendritic cells from monocytes in vitro. *Eur. J. Immunol.* 27:431–441. doi:10.1002/eji.1830270213

Choi, J.H., Y. Do, C. Cheong, H. Koh, S.B. Boscardin, Y.S. Oh, L. Bozzacco, C. Trumpfheller, C.G. Park, and R.M. Steinman. 2009. Identification of antigen-presenting dendritic cells in mouse aorta and cardiac valves. *J. Exp. Med.* 206:497–505. doi:10.1084/jem.20082129

Daro, E., B. Pulendran, K. Brasel, M. Teepe, D. Pettit, D.H. Lynch, D. Vremec, L. Robb, K. Shortman, H.J. McKenna, et al. 2000. Polyethylene glycol-modified GM-CSF expands CD11b(high)CD11c(high) but not

CD11b(low)CD11c(high) murine dendritic cells in vivo: a comparative analysis with Flt3 ligand. *J. Immunol.* 165:49–58.

Ditiatkovski, M., B.H. Toh, and A. Bobik. 2006. GM-CSF deficiency reduces macrophage PPAR-gamma expression and aggravates atherosclerosis in ApoE-deficient mice. *Arterioscler. Thromb. Vasc. Biol.* 26:2337–2344. doi:10.1161/01.ATV.0000238357.60338.90

Geissmann, F., S. Jung, and D.R. Littman. 2003. Blood monocytes consist of two principal subsets with distinct migratory properties. *Immunity.* 19:71–82. doi:10.1016/S1074-7613(03)00174-2

Goto, Y., J.C. Hogg, T. Suwa, K.B. Quinlan, and S.F. van Eeden. 2003. A novel method to quantify the turnover and release of monocytes from the bone marrow using the thymidine analog 5′-bromo-2′-deoxyuridine. *Am. J. Physiol. Cell Physiol.* 285:C253–C259.

Grage-Griebenow, E., H.D. Flad, and M. Ernst. 2001. Heterogeneity of human peripheral blood monocyte subsets. *J. Leukoc. Biol.* 69:11–20.

Hamilton, J.A., and G.P. Anderson. 2004. GM-CSF biology. *Growth Factors.* 22:225–231. doi:10.1080/08977190412331279881

Inaba, K., R.M. Steinman, M.W. Pack, H. Aya, M. Inaba, T. Sudo, S. Wolpe, and G. Schuler. 1992. Identification of proliferating dendritic cell precursors in mouse blood. *J. Exp. Med.* 175:1157–1167. doi:10.1084/jem.175.5.1157

Ishibashi, S., J.L. Goldstein, M.S. Brown, J. Herz, and D.K. Burns. 1994a. Massive xanthomatosis and atherosclerosis in cholesterol-fed low density lipoprotein receptor-negative mice. *J. Clin. Invest.* 93:1885–1893. doi:10.1172/JCI117179

Ishibashi, T., K. Yokoyama, J. Shindo, Y. Hamazaki, Y. Endo, T. Sato, S. Takahashi, Y. Kawarabayasi, M. Shiomi, T. Yamamoto, et al. 1994b. Potent cholesterol-lowering effect by human granulocyte-macrophage colony-stimulating factor in rabbits. Possible implications of enhancement of macrophage functions and an increase in mRNA for VLDL receptor. *Arterioscler. Thromb.* 14:1534–1541.

Jongstra-Bilen, J., M. Haidari, S.N. Zhu, M. Chen, D. Guha, and M.I. Cybulsky. 2006. Low-grade chronic inflammation in regions of the normal mouse arterial intima predisposed to atherosclerosis. *J. Exp. Med.* 203:2073–2083. doi:10.1084/jem.20060245

Kriss, J.P., and L. Revesz. 1962. The distribution and fate of bromodeoxyuridine and bromodeoxycytidine in the mouse and rat. *Cancer Res.* 22:254–265.

Lessner, S.M., H.L. Prado, E.K. Waller, and Z.S. Galis. 2002. Atherosclerotic lesions grow through recruitment and proliferation of circulating monocytes in a murine model. *Am. J. Pathol.* 160:2145–2155.

Lichtman, A.H., S.K. Clinton, K. Iiyama, P.W. Connelly, P. Libby, and M.I. Cybulsky. 1999. Hyperlipidemia and atherosclerotic lesion development in LDL receptor-deficient mice fed defined semipurified diets with and without cholate. *Arterioscler. Thromb. Vasc. Biol.* 19:1938–1944.

Merched, A.J., E. Williams, and L. Chan. 2003. Macrophage-specific p53 expression plays a crucial role in atherosclerosis development and plaque remodeling. *Arterioscler. Thromb. Vasc. Biol.* 23:1608–1614. doi:10.1161/01.ATV.0000084825.88022.53

Moore, K.J., and M.W. Freeman. 2006. Scavenger receptors in atherosclerosis: beyond lipid uptake. *Arterioscler. Thromb. Vasc. Biol.* 26:1702–1711. doi:10.1161/01.ATV.0000229218.97976.43

Mullick, A.E., K. Soldau, W.B. Kiosses, T.A. Bell III, P.S. Tobias, and L.K. Curtiss. 2008. Increased endothelial expression of Toll-like receptor 2 at sites of disturbed blood flow exacerbates early atherogenic events. *J. Exp. Med.* 205:373–383. doi:10.1084/jem.20071096

Nussenzweig, M.C., R.M. Steinman, M.D. Witmer, and B. Gutchinov. 1982. A monoclonal antibody specific for mouse dendritic cells. *Proc. Natl. Acad. Sci. USA.* 79:161–165. doi:10.1073/pnas.79.1.161

Orekhov, A.N., E.R. Andreeva, I.A. Mikhailova, and D. Gordon. 1998. Cell proliferation in normal and atherosclerotic human aorta: proliferative splash in lipid-rich lesions. *Atherosclerosis.* 139:41–48. doi:10.1016/S0021-9150(98)00044-6

Qiao, J.H., J. Tripathi, N.K. Mishra, Y. Cai, S. Tripathi, X.P. Wang, S. Imes, M.C. Fishbein, S.K. Clinton, P. Libby, et al. 1997. Role of macrophage colony-stimulating factor in atherosclerosis: studies of osteopetrotic mice. *Am. J. Pathol.* 150:1687–1699.

Rajavashisth, T.B., A. Andalibi, M.C. Territo, J.A. Berliner, M. Navab, A.M. Fogelman, and A.J. Lusis. 1990. Induction of endothelial cell expression of granulocyte and macrophage colony-stimulating factors by modified low-density lipoproteins. *Nature.* 344:254–257. doi:10.1038/344254a0

Rosas, M., S. Gordon, and P.R. Taylor. 2007. Characterisation of the expression and function of the GM-CSF receptor alpha-chain in mice. *Eur. J. Immunol.* 37:2518–2528. doi:10.1002/eji.200636892

Rosenfeld, M.E., and R. Ross. 1990. Macrophage and smooth muscle cell proliferation in atherosclerotic lesions of WHHL and comparably hypercholesterolemic fat-fed rabbits. *Arteriosclerosis.* 10:680–687.

Shaposhnik, Z., X. Wang, M. Weinstein, B.J. Bennett, and A.J. Lusis. 2007. Granulocyte macrophage colony-stimulating factor regulates dendritic cell content of atherosclerotic lesions. *Arterioscler. Thromb. Vasc. Biol.* 27:621–627. doi:10.1161/01.ATV.0000254673.55431.e6

Skålén, K., M. Gustafsson, E.K. Rydberg, L.M. Hultén, O. Wiklund, T.L. Innerarity, and J. Borén. 2002. Subendothelial retention of atherogenic lipoproteins in early atherosclerosis. *Nature.* 417:750–754. doi:10.1038/nature00804

Smith, J.D., E. Trogan, M. Ginsberg, C. Grigaux, J. Tian, and M. Miyata. 1995. Decreased atherosclerosis in mice deficient in both macrophage colony-stimulating factor (op) and apolipoprotein E. *Proc. Natl. Acad. Sci. USA.* 92:8264–8268. doi:10.1073/pnas.92.18.8264

Smith, M.L., T.S. Olson, and K. Ley. 2004. CXCR2- and E-selectin–induced neutrophil arrest during inflammation in vivo. *J. Exp. Med.* 200:935–939. doi:10.1084/jem.20040424

Swirski, F.K., M.J. Pittet, M.F. Kircher, E. Aikawa, F.A. Jaffer, P. Libby, and R. Weissleder. 2006. Monocyte accumulation in mouse atherogenesis is progressive and proportional to extent of disease. *Proc. Natl. Acad. Sci. USA.* 103:10340–10345. doi:10.1073/pnas.0604260103

Swirski, F.K., P. Libby, E. Aikawa, P. Alcaide, F.W. Luscinskas, R. Weissleder, and M.J. Pittet. 2007. Ly-6Chi monocytes dominate hypercholesterolemia-associated monocytosis and give rise to macrophages in atheromata. *J. Clin. Invest.* 117:195–205. doi:10.1172/JCI29950

Tacke, F., D. Alvarez, T.J. Kaplan, C. Jakubzick, R. Spanbroek, J. Llodra, A. Garin, J. Liu, M. Mack, N. van Rooijen, et al. 2007. Monocyte subsets differentially employ CCR2, CCR5, and CX3CR1 to accumulate within atherosclerotic plaques. *J. Clin. Invest.* 117:185–194. doi:10.1172/JCI28549

Xu, H., R. Dawson, J.V. Forrester, and J. Liversidge. 2007. Identification of novel dendritic cell populations in normal mouse retina. *Invest. Ophthalmol. Vis. Sci.* 48:1701–1710. doi:10.1167/iovs.06-0697